International Journal of Innovations & Research Analysis (IJIRA)
ISSN :2583-0295, Impact Factor: 5.449, Volume 03, No. 04(I), October- December, 2023, pp 39-56

DC SIDE FAULT DETECTION AND CHARACTERIZATION IN PV ARRAY BY INTRODUCING THE ELECTRICAL FAULT PARAMETERS

Abhishek Kumar Gupta*
Rajveer Singh**
Sanjiv Kumar***

ABSTRACT

Photovoltaic energy is the one amid the other non-conventional energy resources extensively used. The convenient conversion process makes it more advantageous. The unusual situation like partial shading and faults are major cause for limiting the power below maximum possible power from the photovoltaic array. In order to operate and maintain a photovoltaic plant safely, effective fault detection and diagnosis are essential. Recent advances in fault diagnosis have been made through the use of machine learning methods. Although, some limitations remain such as feature extraction depends on expert expertise and is not automated. The second problem is that artificial characteristic extraction ignores some features that could be useful. Third, shallow network structures can't be used to learn the nonlinear characteristics of current-voltage curves. These issues are addressed by applying supervised deep learning methods that can automatically extract features, but a lot of categorized data is needed. This article proposed a fault detection scheme based on the voltage and current parameters. The voltage and current ratios are introduced to measure the threshold values according to various faults behaviour. This technique requires less data to detect the fault and also characterise the faults automatically. The wavelet packet transform is used to analyse and measure the energy and standard deviation (STD) of the proposed PV fault parameters. The simulated results have also been analysed using wavelet packet transform (WPT). The performance evaluation and the testing of proposed fault detection scheme is done using 4×4 PV array of 1596 W in MATLAB/Simulink.

Keywords: *Fault Detection, Fault Diagnosis, Photovoltaic Array, Partial Shading, Wavelet Packet Transform.*

Introduction

In recent years as well as in current time, the photovoltaic systems are best method to utilize the solar energy directly and in coming years it will become more popular due to new technologies, unavailability of conventional sources and reduction in material cost [1]. In the solar power plants, the fault analysis is the primary concern of the researchers to increase the output energy, system reliability and also to maintain the safety. The lack of protection may cause the photovoltaic system faults which results the breakdown in photovoltaic module, wires, etc. Photovoltaic have current-limiting and non-linear output characteristics due to which under some special cases the over current protection devices are not able to clear the faults in photovoltaic array. Such faults may lead to risk of dc arcing and fire [2]. The fire hazard occurred because of ground fault on multiple points in a 383 kW solar system in Bakersfield, California in 2009. One more fire hazard was reported, it occurred due to line-line faults in photovoltaic array in a solar power system in California [2]–[4].

* Department of Electrical Engineering, Jamia Millia Islamia, New Delhi, India.
** Department of Electrical Engineering, Jamia Millia Islamia, New Delhi, India.
*** Department of Electrical Engineering, Government Polytechnic, Shahbad, Rampur, U.P., India.

According to U. S. National Electrical Code, the conventional fault protection devices are arc-fault circuit interrupters, over current protection devices (OCPD) and ground fault protection devices (GFPD) [5]. These devices are capable of remove the faults and disconnect the system from the faulty sub-systems. But these protection devices operate only in case of large current flow due to faults [6], [7]. Basic reason of faults in aquatic PV module like open-circuit faults due to damaged PV cells and joint failure, short-circuit faults due to line to line and/or line to ground connections are reported in [8]. Independent of the PV module interconnections, the I-V curve is used in [9] for the performance evaluation of PV array under different fault conditions. A data driven technique for detection of fault and its classification has been proposed in [10], where I-V curve has been used to evaluate the normal and faulty conditions of PV module. Degradation causes the mismatch of photovoltaic module and partial shading of photovoltaic module causes power losses and black spots on module reported in [11]–[16]. Different array reconfiguration procedure reported in [17], [18] to minimize the power losses during partial shading. Also, a new reconfiguration procedure has been proposed called two phase array reconfigurations. According to literatures, artificial neural network and fuzzy system are commonly used techniques for detection of fault due to PV array shading [19], [20]. The abnormal conditions occurred in photovoltaic system like various faults and shading on PV cells are major cause to minimization of maximum power available at the PV terminals. Based on ensemble learning, a fault diagnosis technique is proposed in [21]. Only two types of faults (short-circuit and partial shading) can be detected using this technique. Solar irradiation, cell temperature, ambiance temperature and output power of PV array are required to diagnose the faults.

In this research work, a novel algorithm has been proposed to detect and diagnose the three different types of the electrical faults that usually occur in a PV array. The proposed algorithm is based on three parameters like solar irradiation, voltage and current of the PV terminal. The energy of the different fault indicators is also analysed using wavelet packet transform (WPT).

Further this paper is organised as follows: The PV array under various fault conditions, different fault detection scheme and a novel fault detection and characterization technique are presented in section 2, 3 and 4 respectively. In section 5, the results of proposed technique are discussed for different fault conditions. At last, in section 6, the research work is concluded.

Photovoltaic Array under Various Faults

A PV array with combination of four parallel and four series module is modelled in MATLAB/Simulink for the further fault detection and characterization. The electrical specification of single PV module is given in table 1.

Table 1: Nexpower Technology NH-100 UT_4A solar panel electrical specification at STC

Parameter	Value
Maximum output power	99.75 W
Voltage at MPP (V_{mp})	37.5 V
Current at MPP (I_{mp})	2.66 A
Open-circuit voltage (V_{oc})	50.5 V
Short-circuit current (I_{sc})	3.3 A
Temperature coefficient of (V_{oc})	-0.306 %/ ^{o}C
Temperature coefficient of (I_{sc})	0.09 %/ ^{o}C
Shunt resistance (R_{sh})	77.04 ohm
Series resistance (R_{se})	2.74 ohm

In the solar power plants, faults may be classified as the permanent and temporary faults. The permanent faults in photovoltaic plants are line-line fault, line-ground fault, mismatch fault and open-circuit fault. These faults lead to the reduction in generation of PV power permanently. Partial shading of PV array is the example of temporary faults in photovoltaic plants. Among these faults, line-line and line-ground fault happens due to causeless connection between line to line or one or more line of photovoltaic array and ground i.e. short circuiting of two nodes of different potential [23]. Various faults in PV array is shown in figure 2. Fa_1 and Fa_2 are the LL fault with one and two module mismatched respectively. Fb_1 and Fb_2 are LG and LLG faults respectively. Fc_1 is open-circuit fault in first column and Fc_2 is open-circuit fault in second column. Partial shading condition is shown in figure 2 (d) and two sample of shading pattern is given in table 2 and 3.

Based on the data in Table 1, a PV array of 16 PV modules (4×4) has been modelled in MATLAB/Simulink. The array maximum output power at standard test condition (STC) is 1596 W.

Table 2: Shading pattern for PSC 1

1000	1000	1000	1000
1000	1000	1000	1000
800	800	800	800
700	700	700	700

Table 3: Shading pattern for PSC 2

900	900	900	900
700	700	700	700
500	500	500	500
300	300	300	300

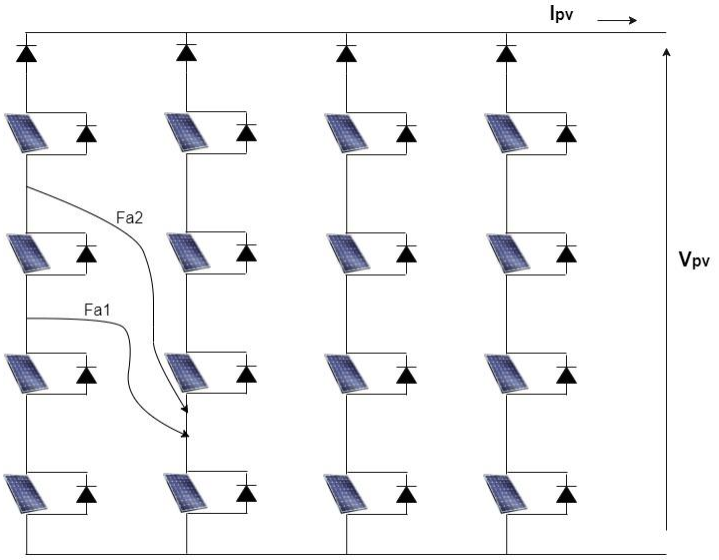

(a)

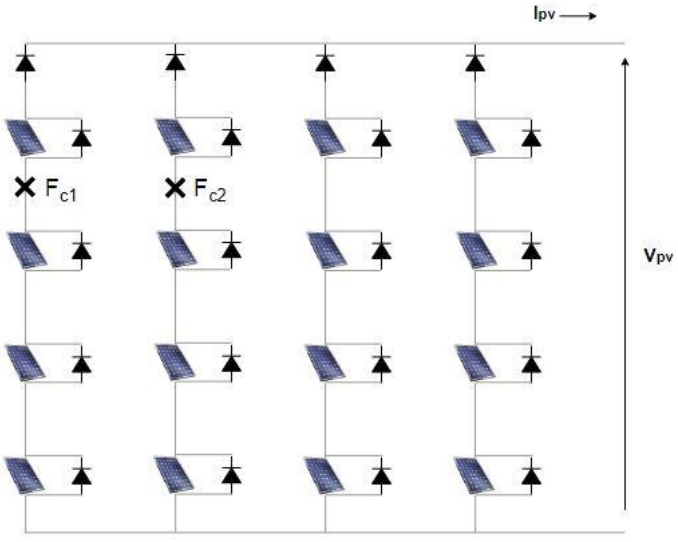

(c)

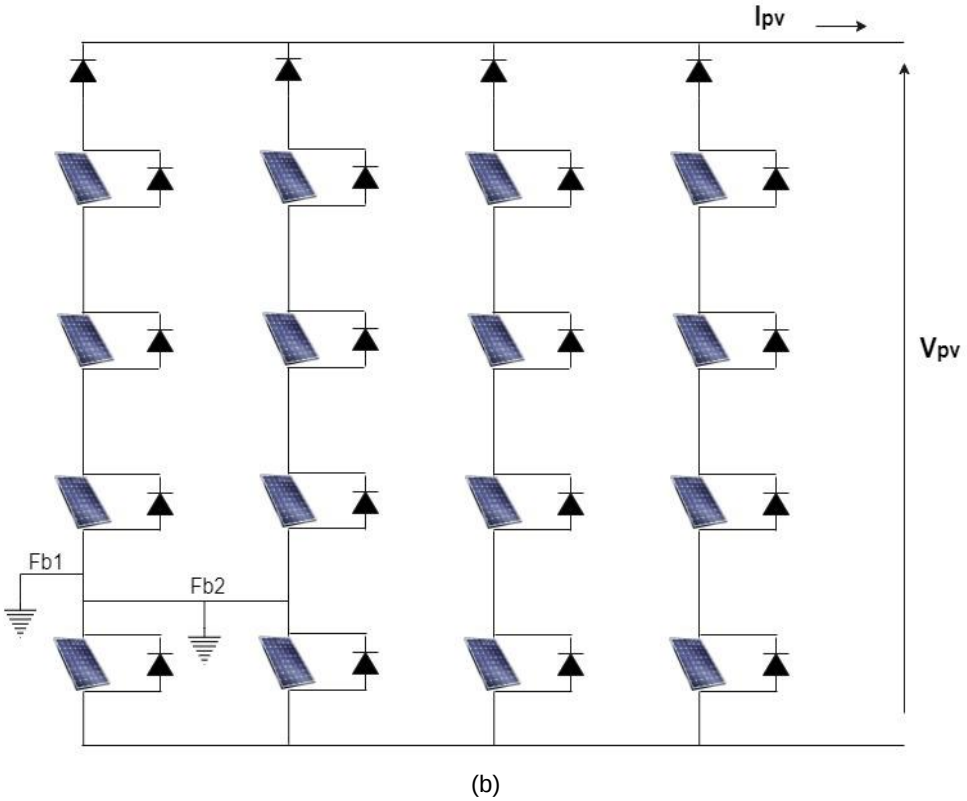

(b)

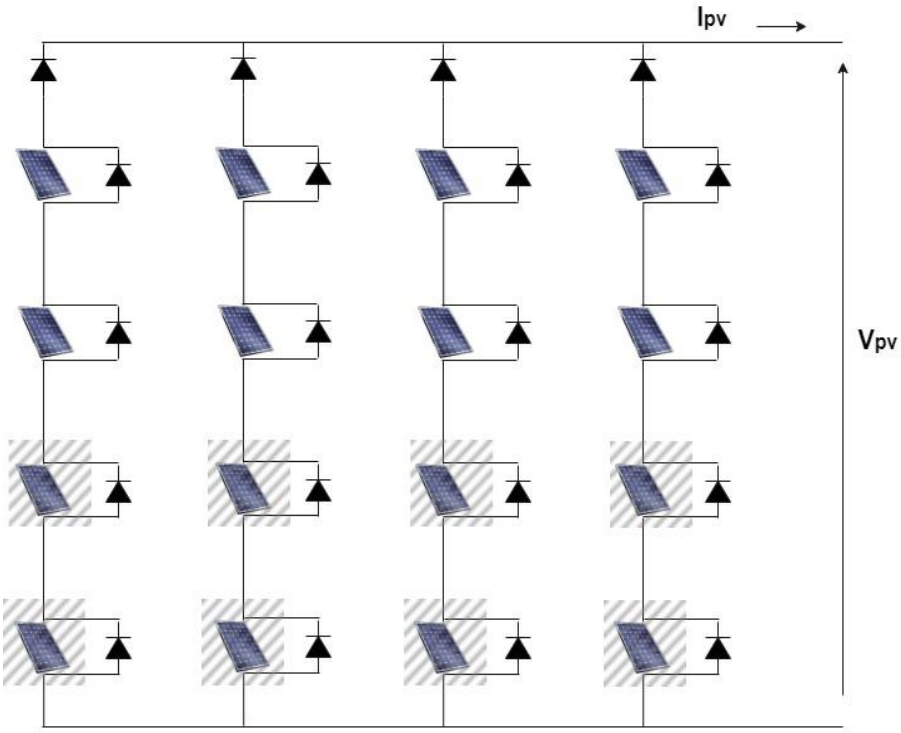

(d) Figure 2: (a) Line-line fault, (b) Line-ground fault, (c) Open-circuit fault, (d) Partial shading

Proposed Fault Detection Scheme

In this paper, several faults like, line-line fault, line-ground fault, open-circuit fault and shading of the photovoltaic array of proposed PV generation system (shown in figure 3) are considered for the faults detection and diagnosis algorithm.

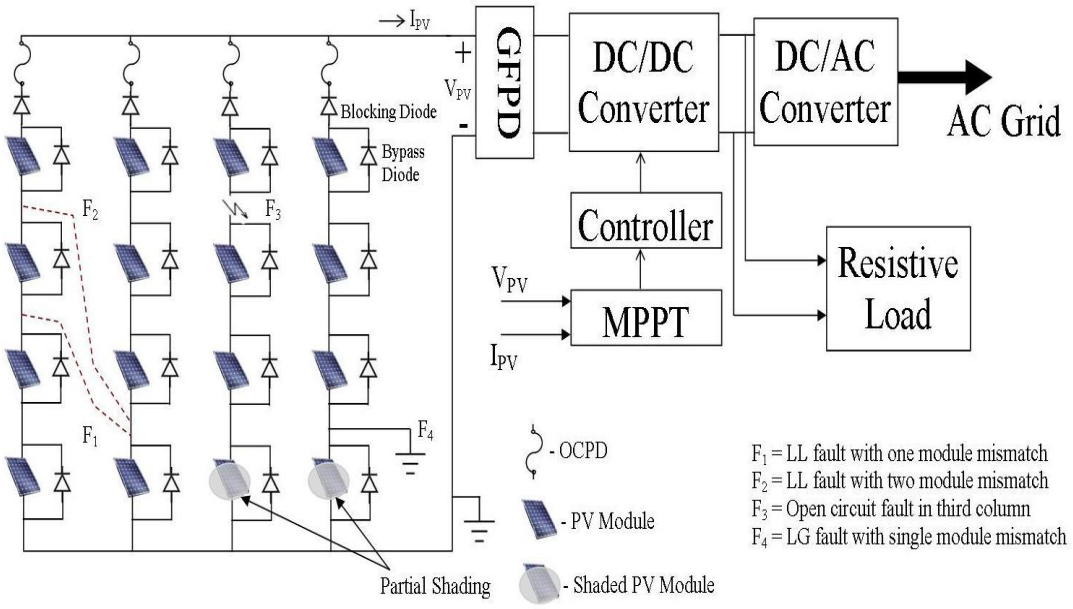

Figure 3: Block diagram of a PV generation system with various fault conditions

For the purpose of detection of faults, the voltage ratio (α) and current ratio (β) are introduced. The ratios α and β are defined as:

$$\alpha = \frac{\mathrm{V}}{\mathrm{V_{oc}}} \tag{19}$$

$$\beta = \frac{\mathrm{I}}{\mathrm{I_{sc}}} \tag{20}$$

Here, V and I are the terminal voltage and load current respectively; V_{oc} and I_{sc} are the voltage and current parameters at no-load and short-circuit conditions respectively. The V_{oc} and I_{sc} can be obtained by [24]:

$$I_{sc} = N_p\left[\frac{I_{scSTC}}{1000}G + k_i(T - T_{STC})\right] \tag{21}$$

$$V_{oc} = N_s[V_{ocSTC} + k_v(T - T_{STC}) + V_t \ln\left(\frac{I_{sc}/N_p}{I_{scSTC}}\right)] \tag{22}$$

The PV output parameters are lesser dependent of temperature variations compared to irradiation variations [25], so equations (21) and (22) can be rewritten as:

$$I_{sc} = N_p\left[\frac{I_{scSTC}}{1000}G\right] \tag{23}$$

$$V_{oc} = N_s[V_{ocSTC} + V_t \ln\left(\frac{I_{sc}/N_p}{I_{scSTC}}\right)] \tag{24}$$

From equation (19) and (20), if the PV system is operating in healthy condition, then the voltage and current ratios can be written as:

$$\alpha_{\mathrm{m}} = \frac{\mathrm{V_{mpp}}}{\mathrm{V_{oc}}} \tag{25}$$

$$\beta_{\mathrm{m}} = \frac{\mathrm{I_{mpp}}}{\mathrm{I_{sc}}} \tag{26}$$

In a healthy PV array, the V_{mpp} and I_{mpp} can be obtained as follows [25]:

$$I_{mpp} = N_p \left[\frac{I_{mpSTC}}{1000} G + k_i (T - T_{STC})\right] (27)$$

$$V_{mpp} = N_s \left[V_t \ln\left(1 + \left(\frac{I_{sc} - I_{mpp}}{I_{sc}}\right)\left(e^{\frac{V_{oc}}{N_s V_t}} - 1\right)\right) - \frac{I_{mpp}}{N_p} R_s\right] \quad (28)$$

Determination of Threshold Values

The two proposed variable α and β (in section 3) used to define the threshold values. In this section, threshold values for various faults in PV array like line-line fault, line-ground fault, open-circuit fault and partial shading conditions have been discussed.

- **Line-Line and Line-Ground Faults**

In a grounded system, the behaviour of short-circuit fault and line-line fault is same. Also the PV parameter variations are same for LL and LG faults [2], [26]. When a line-line fault occurred in a PV string, then the decreased value of output voltage depends on the mismatch level (i.e. the number of module mismatched). Similarly, for line-ground faults it depends on the voltage of module between the fault point and ground. In such faults condition the voltage ratio can be obtained by:

$$\alpha_{\mathrm{LL/LG}} = \left(1 - \frac{1}{\mathrm{N_s}}\right)\frac{V_{mpp}}{V_{oc}} = \gamma \alpha_{\mathrm{m}} \quad (29)$$

Where, $\gamma = 1 - \frac{1}{\mathrm{N_s}}$

Hence, the threshold value for the detection of faults in case of LL/LG faults is given by:

$$Th_{LL/LG} = \gamma \alpha_{\mathrm{m}} \pm \varepsilon \quad (30)$$

Where, ε is the percentage threshold range, ε = ±2%.

- **Open Circuit Faults**

The decreased value of output current in case of an open-circuit fault in a PV string depends on the current of the faulty line (i.e. it reduced by current of that array). During this situation, the current ratio can be obtained by:

$$\beta_{\mathrm{oc}} = \left(1 - \frac{1}{\mathrm{N_p}}\right)\frac{I_{mpp}}{I_{sc}} = \lambda\, \beta_{\mathrm{m}} \quad (31)$$

Were, $\lambda = 1 - \frac{1}{\mathrm{N_p}}$

Hence, the threshold value for open-circuit fault detection is given by:

$$Th_{oc} = \lambda \beta_{\mathrm{m}} \pm \varepsilon \quad (32)$$

- **Partial Shading Faults**

The partial shading fault is characterised as temporary fault. Such faults are very common in PV generation system. Less current produces by the shaded cell so the power generates from that module is lower than other modules [27]–[29]. In such case the voltage and current ratios are obtained as:

$$\alpha_{\mathrm{PSC}} = \frac{\mathrm{V_{mp}}}{\mathrm{V_{oc}}} (33)$$

$$\beta_{\mathrm{PSC}} = \frac{\mathrm{I_{mp}}}{\mathrm{I_{sc}}} \quad (34)$$

In case of partial shading the V_{mp} and I_{mp} are the MPP values from the photovoltaic array with peak irradiation (G_{mp}). Hence, the V_{mp} and I_{mp} for partial shading can be obtained same as equation (27) and (28) by replacing G by G_{mp}, V_{mpp} by V_{mp} and I_{mpp} by I_{mp}.

Hence, the threshold value for the detection of faults in case of partial shading faults is given by:

$$Th_{PSC} = \left(\frac{\mathrm{I_{mp}}}{\mathrm{I_{sc}}}\right) \pm \varepsilon = \beta_{\mathrm{PSC}} \pm \varepsilon \quad (35)$$

Based on the discussion about the threshold values, a flowchart have been developed, shown in figure 4.

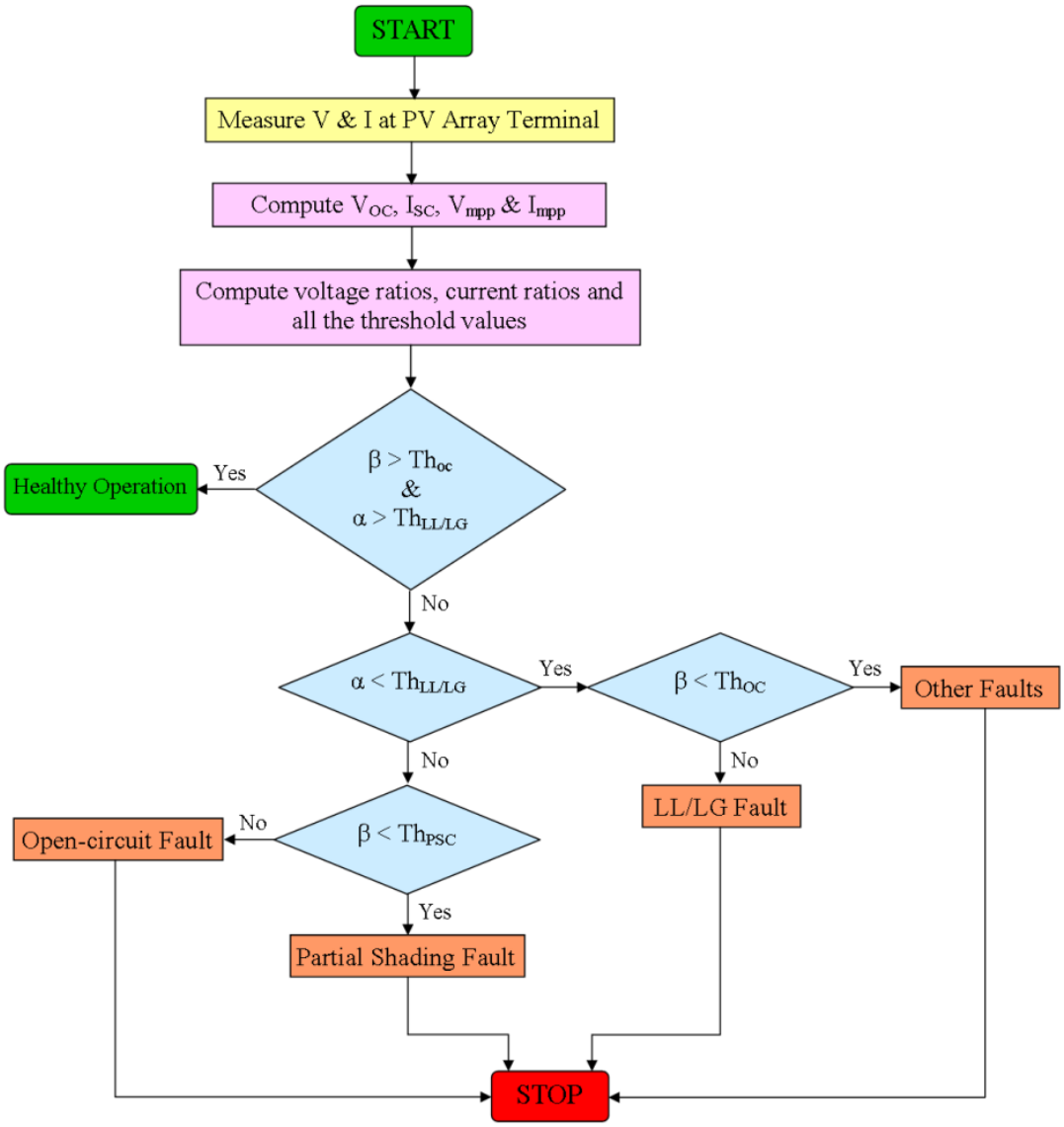

Figure 4: Flow chart of the proposed fault detection technique

Results and Discussion

In order to get the results of the proposed technique of fault detection, a PV generation system with 1596 W is developed on the MATLAB/Simulink. The structure of the modelled system is shown in figure 3. The electrical parameters of the PV module are given in Table 1.

- **Healthy (fault free) Operation**

Healthy operation in the PV system is the very much desired operation. The voltage and current parameter ratios of healthy operation are shown in figure 5 and figure 6. During this observation the test condition taken are 25 ^{0}C temperature and 1000 W/m^2 irradiation. Figure 5 shows voltage ratios (α and α_m), and the threshold of LL/LG faults ($Th_{LL/LG}$). Figure 6 shows the current ratios (β and β_m), and the threshold of OC and PSC faults ($Th_{OC}$and Th_{PSC}). It can be seen in figure 5, $Th_{LL/LG}$is lower to the α, means the PV system is operating without LL/LG faults. In figure 6, β exceeds the Th_{OC} and Th_{PSC} i.e. the PV system is free from open circuit fault and partial shading.

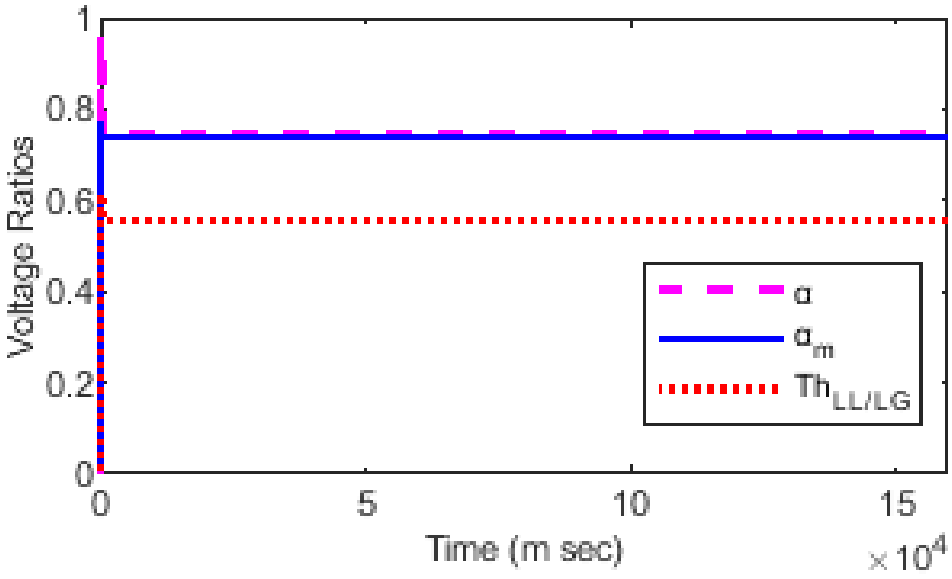

Figure 5: Voltage Ratios of Healthy Operation

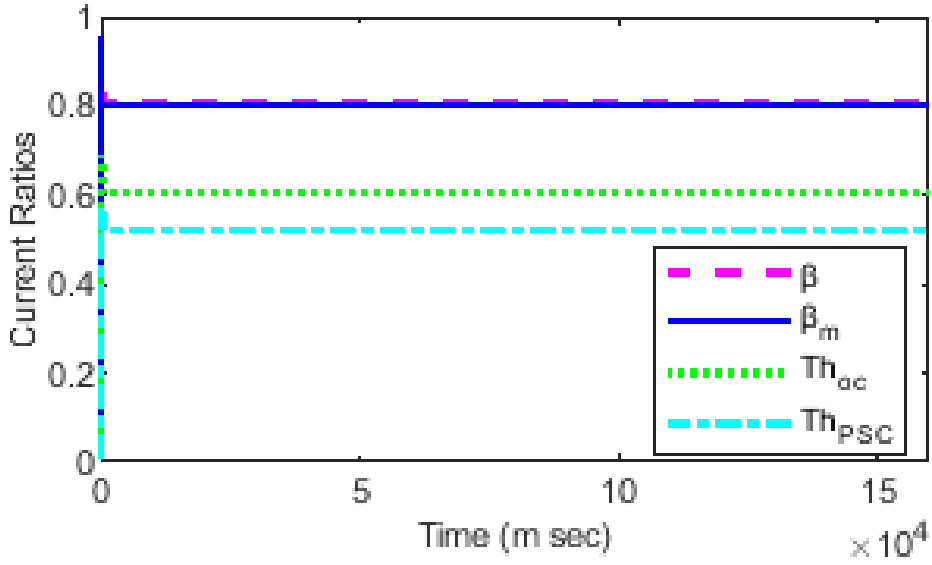

Figure 6: Current ratios of Healthy Operation

- **Line-Line/Line-Ground Fault Operation**

Line-ground fault is special case of line-line fault. The behaviour of both the faults is identical. The voltage and current ratios of fault case F_{a2} (figure 2 (a)) is shown in figure 7 and figure 8. LL/LG faults are basically the unusual connection between the two or more different potential nodes, so in such case the voltage of the PV system decreases. The voltage of the PV string is decreased by the summation of the voltages of the mismatched PV module. So, α is lower than the $Th_{LL/LG}$ as shown in figure 7, i.e. the PV array is operating under LL/LG fault. Figure 8 shows that the PV system is free from the open circuit and partial shading faults.

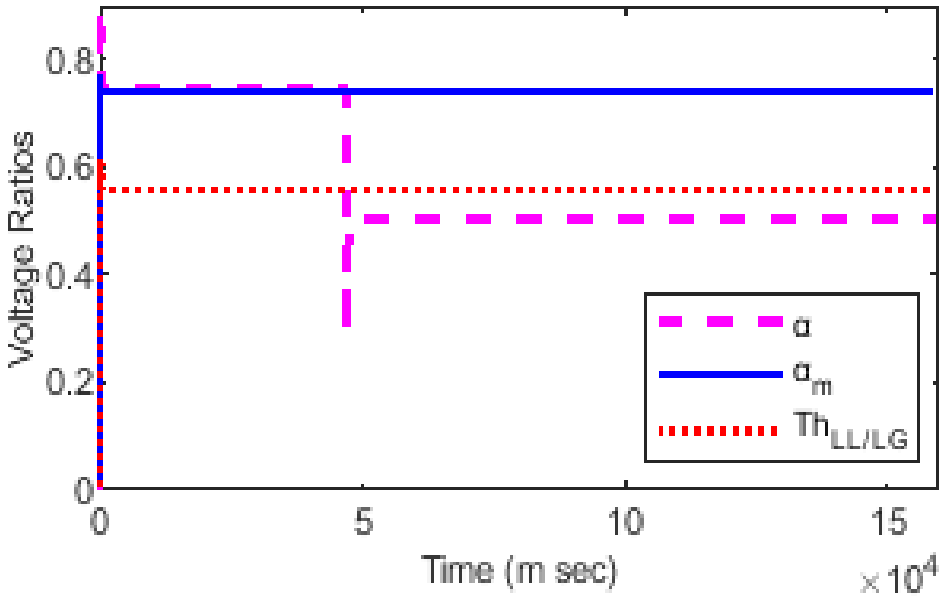

Figure 7: Voltage Ratios of LL/LG Fault

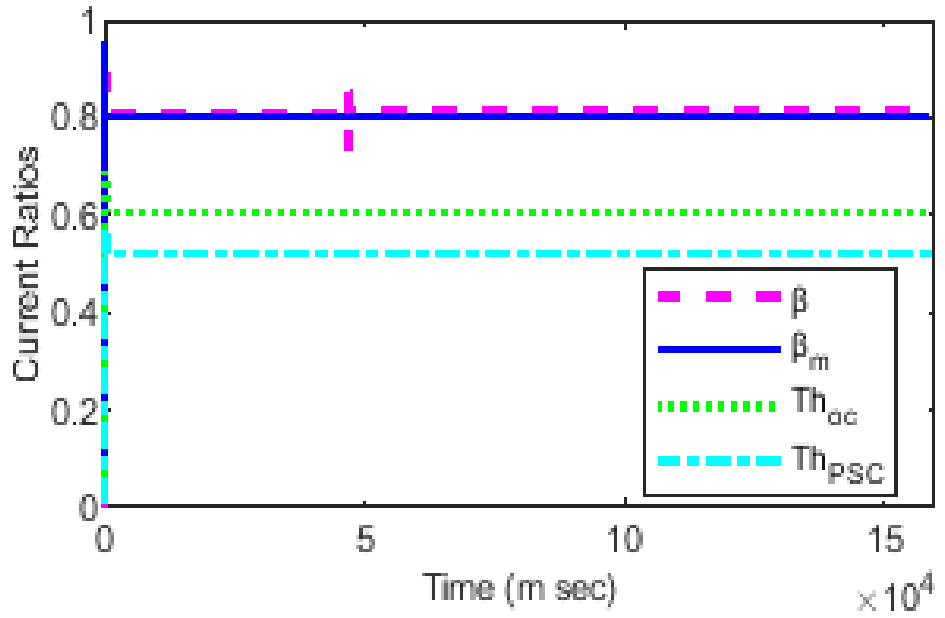

Figure 8: Current Ratios of LL/LG Fault

Open-circuit Fault Operation

The open circuit fault case is shown in figure 2 (c). Fc1 and Fc2 are open circuit faults in PV string 1 and 2 respectively. The voltage and current ratios with the corresponding threshold are shown in figure 9 and figure 10. It can be seen from figure 9, α is greater than the $Th_{LL/LG}$ during the operation. So, the PV system is free from LL/LG faults. But as shown in figure 10, β is less than the Th_{oc} and greater than the Th_{PSC}, means the PV system is operating with the open-circuit fault in at least one of the PV strings.

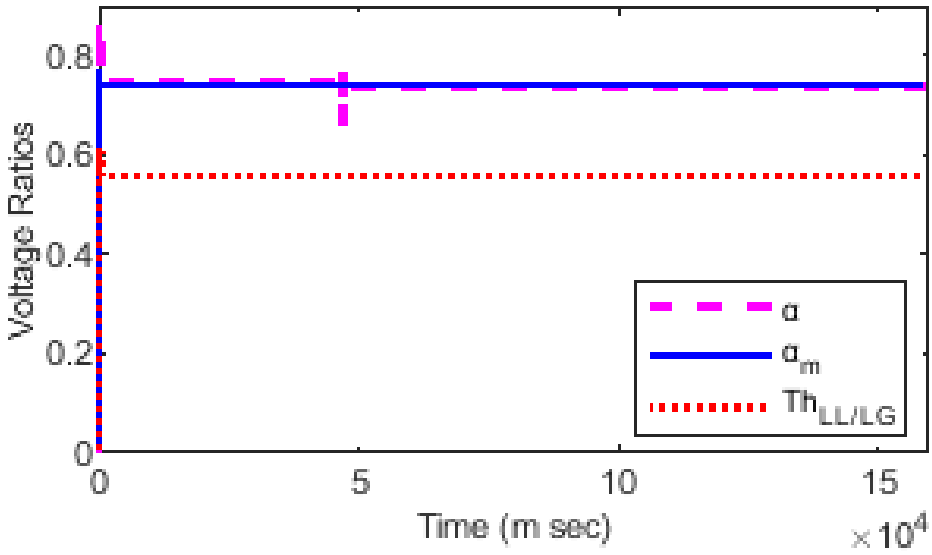

Figure 9: Voltage ratios of open circuit fault

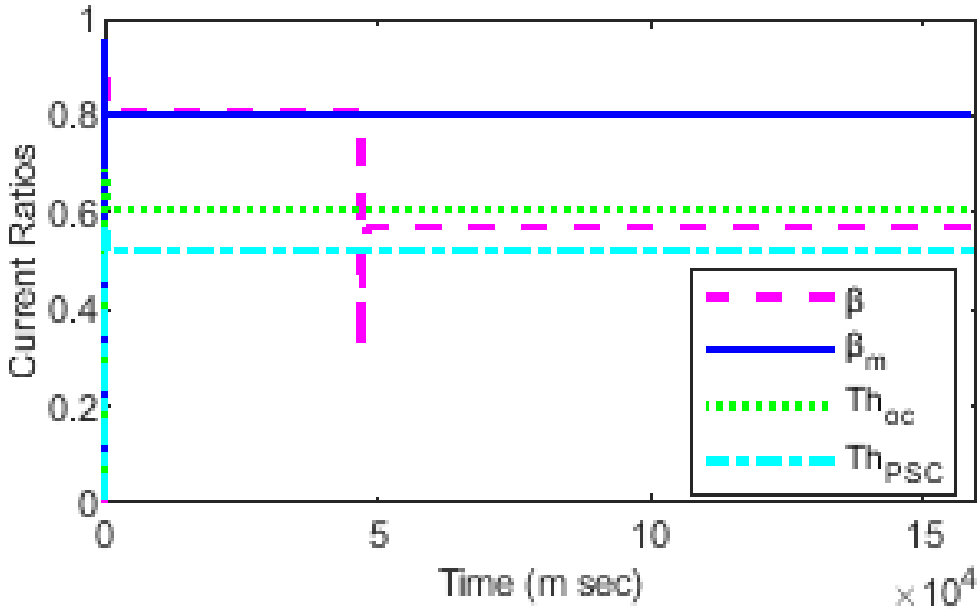

Figure 10: Current ratios of open circuit fault

- **Partial Shading Fault**

In case of partial shading, some portion of the installed PV array is shaded for some time by any means and the rest part get the full irradiation as shown in figure 2 (d). For partial shading of PV array the shading pattern considered is given in table 2. It can be seen from figure 11, α is greater than the $Th_{LL/LG}$ during the operation. So, the PV system is free from LL/LG faults. In figure 12, β is less than the Th_{oc} as well as Th_{PSC}, means the PV system is operating with the partial shading fault.

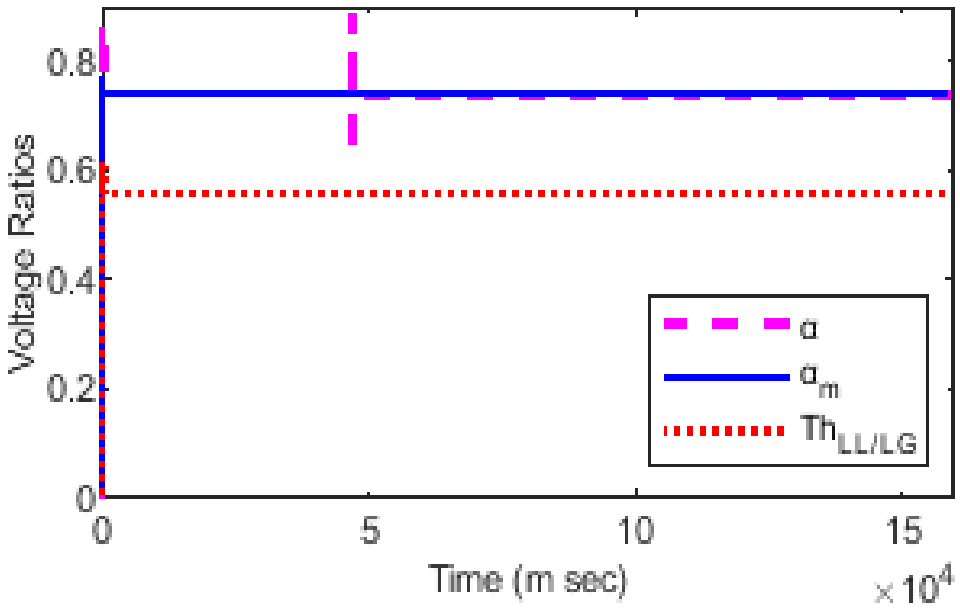

Figure 11: Voltage ratios of partial shading fault

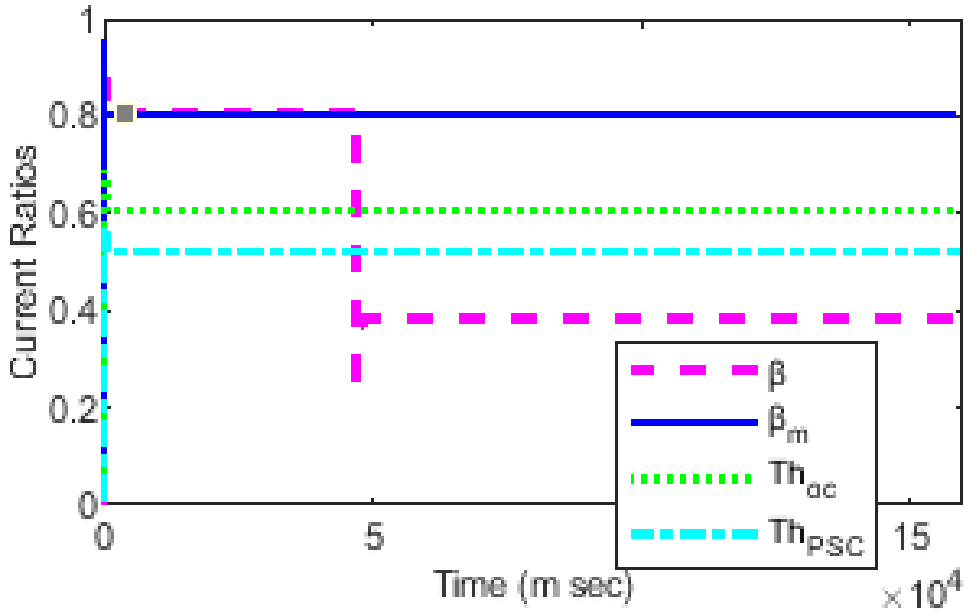

Figure 12: Current ratios of partial shading fault

Table 4: PV Parameters under different Fault Conditions

Type of fault	α	α_m	β	β_m	$Th_{LL/LG}$	Th_{oc}	Th_{PSC}
Fault free	0.7425	0.7425	0.8060	0.8060	0.5568	0.6050	0.5210
LL/LG fault	0.5022	0.7425	0.8113	0.8060	0.5568	0.6050	0.5210
Open-circuit fault	0.7393	0.7425	0.5700	0.8060	0.5568	0.6050	0.5210
Partial shading fault	0.7373	0.7425	0.3842	0.8060	0.5568	0.6050	0.5210

The simulation results of fault variable is discussed and presented in table 4. The analysis of fault variable (*α*&*β*) using wavelet packet transform is given and discussed below. The fault detection and classification technique proposed in section 5 and figure 4 are tested using MATLAB/Simulink software. The simulated data of signal *α* and *β* gone through the WPT so that STD and energy are measured. The measured energy is shown in figure 13-20 for different PV operating conditions and STD and energy is summarised in table 5. The mean value of energy signal during fault free operation is much lower than the mean value of energy signal during faulty operation.

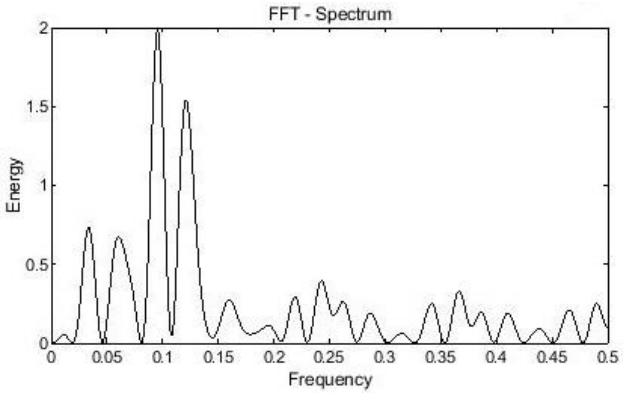

Figure 23: Energy of *α* during healthy PV operation

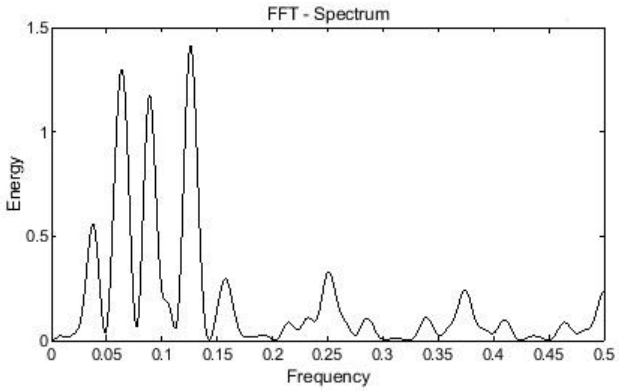

Figure 34: Energy of *β* during healthy PV operation

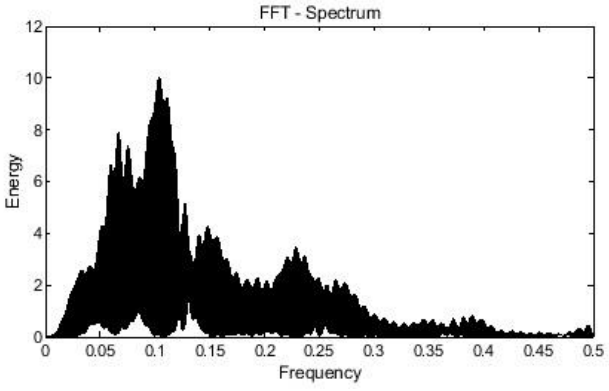

Figure 45: Energy of *α* during LL/LG fault

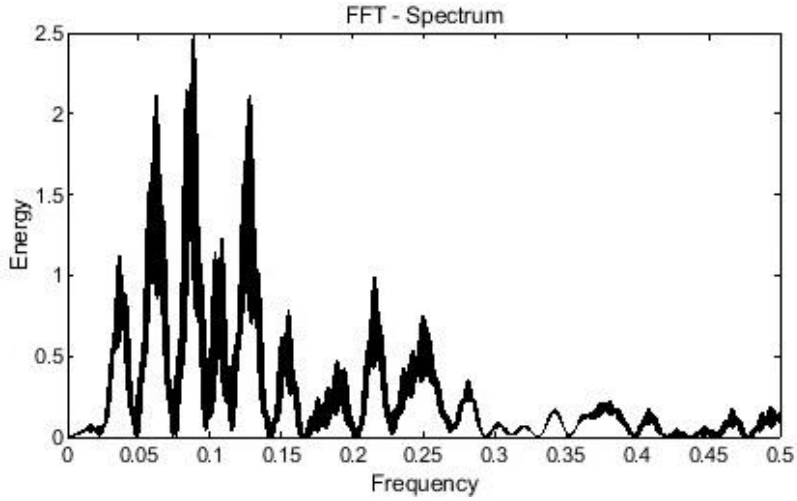

Figure 56: Energy of β during LL/LG fault

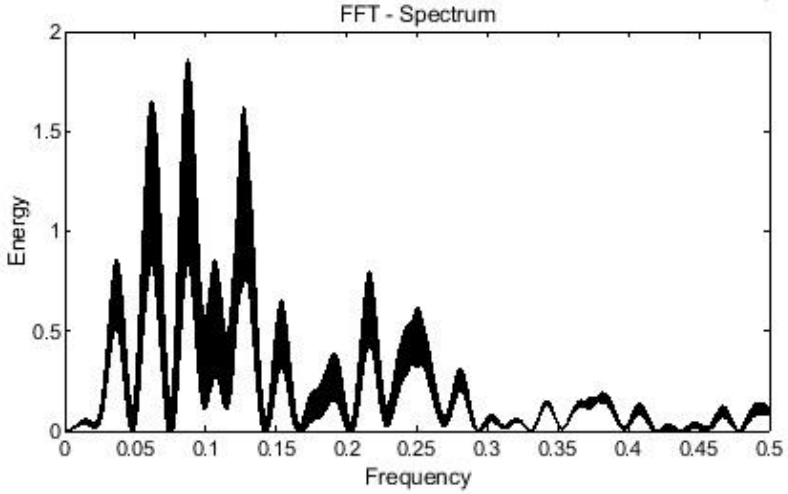

Figure 67: Energy of α during OC fault

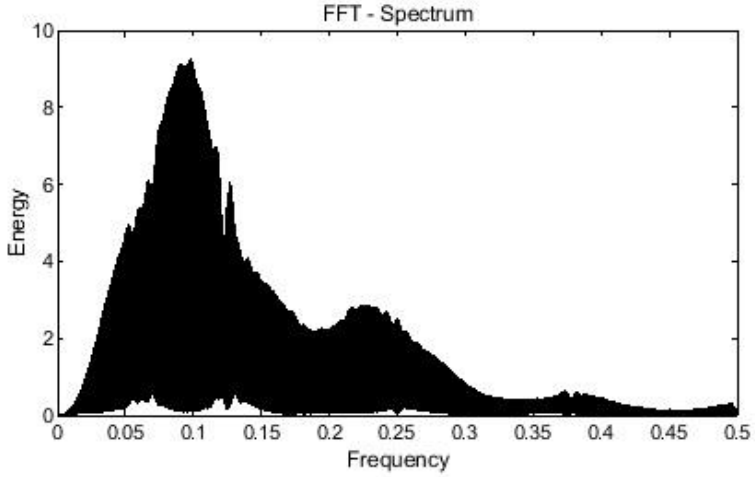

Figure 79: Energy of β during OC fault

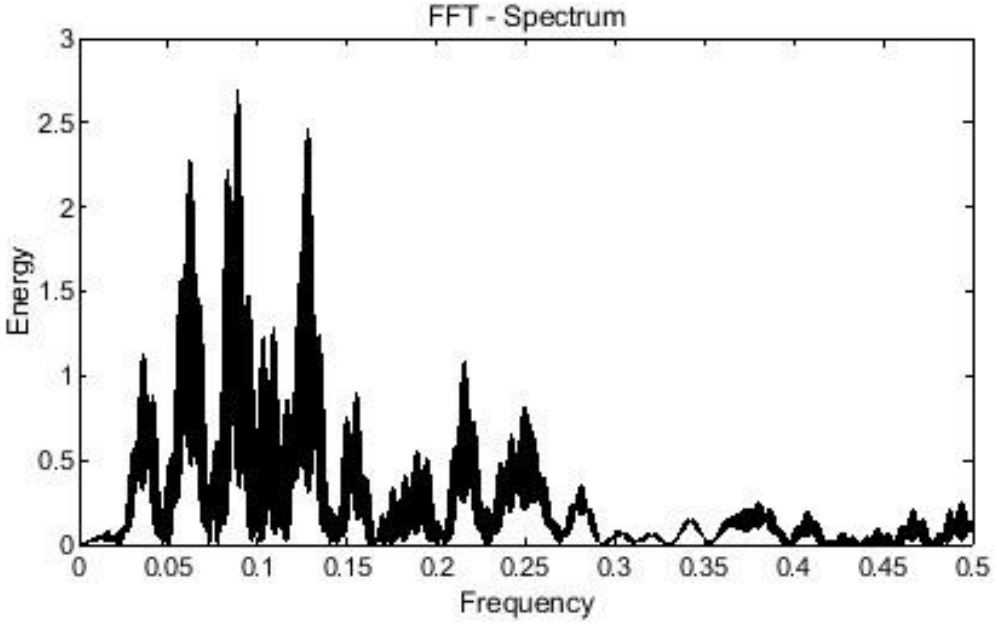

Figure 89: Energy of *α* during partial shading fault

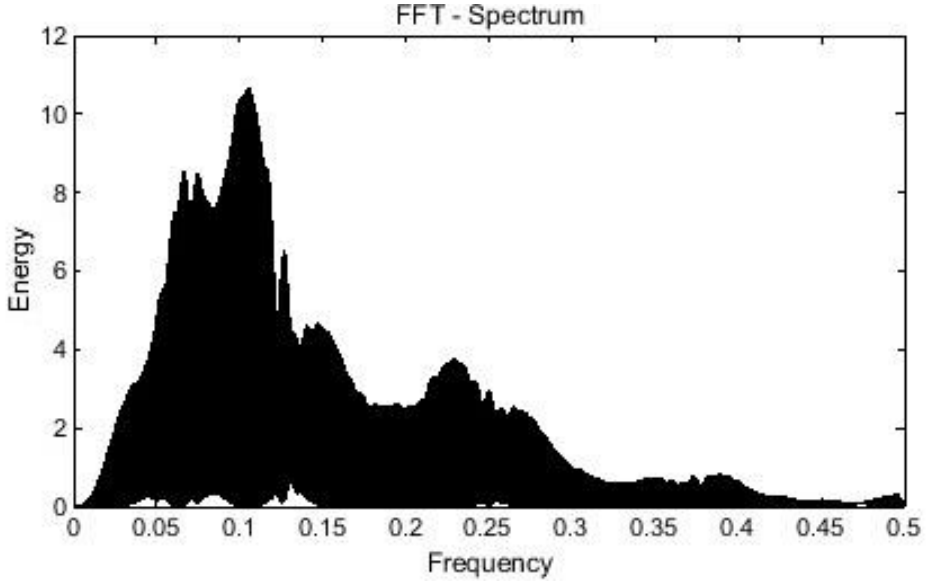

Figure 209: Energy of *β* during partial shading fault

Table 5: STD and energy of different fault conditions using WPT

Types of fault	Fault Variables	STD	Mean
Fault free	*α*_FF	0.001214	0.000326
	*β*_FF	0.001073	0.000299
LL/LG fault	*α*_LL/LG	0.002722	0.006332
	*β*_LL/LG	0.001308	0.003234
Open-circuit fault	*α*_OC	0.001217	0.003091
	*β*_OC	0.002743	0.006312
Partial shading fault	*α*_PSC	0.001278	0.003097
	*β*_PSC	0.002922	0.006323

Table 6: Comparison with the recent PV faults detection techniques

Reference	Fault Type	Method	Parameters Required	Fault Classification	Accuracy	Complexity
[30]	Permanent fault, Partial shading	Difference Measurement	V, I, G	2	High	High
[31]	PV module fault, Partial shading, MPPT Fault	Difference Measurement	V, I, G, T	3	Low	High
[32]	Short circuit, Open circuit, Partial shading, Degradation	Machine Learning	V, I, G, T	4	High	High
[33]	LL fault, Partial shading	Signal Processing	V, I, G	2	High	Low
[34]	LL fault, Partial shading, Abnormal aging	Machine Learning	V, I, G, T	3	High	High
[35]	LL fault, Partial shading, Degradation, Bypass diode fault	Machine Learning	V, I, G	4	High	High
Proposed Technique	LL/LG fault, Open circuit fault, Partial shading	Difference Measurement	V, I, G	4	High	Low

Different PV fault detection techniques have already been discussed in section 1. In **Error! Reference source not found.**, some recent techniques are compared with the proposed technique. The comparison is being evaluated on many parameters like type of fault, method of fault detection, parameters required to detect the faults, accuracy, and complexity of the technique. Based on these parameters, it can be concluded that the proposed technique is comparatively simple and efficient and require less data to detect and diagnose the faults in the PV array.

Conclusion

The various faults have been considered and employed for the fault analysis, detection and its identification. A fault detection technique has been proposed in section 4. This technique is based on the voltage and current ratios. The proposed flowchart (figure 4) is useful to identify the types of faults occurred at PV array such as LL/LG (short-circuit) fault, open-circuit fault and partial shading. The energy signal of various voltages and current ratios have also been analysed using WPT and results are summarised in table 4 and 5. This fault detection algorithm is applied to the modelled PV generation system and found that the proposed fault detection technique is able to detect and identify the fault. The proposed PV fault detection technique has also been compared with the various PV faults detection techniques available in literature as shown in table 6 and found that the proposed PV fault detection technique is simple, efficient and require small amount of data comparatively.

Declaration of Interests

The authors declare that they have no known competing financial interests or personal relationships that could have appeared to influence the work reported in this paper.

Abbreviation

V_{mpp} = voltage at MPP of healthy PV array

I_{mpp} = current at MPP of healthy PV array

I_{mpSTC} = I_{mpp} at STC

α = voltage ratio

β = current ratio

α_m = voltage ratio at MPP

β_m = current ratio at MPP

α_{sc} = short-circuit voltage ratio

$Th_{LL/LG}$ = threshold value for LL/LG fault

Th_{PSC} = threshold value for partial shading fault

V_t = thermal voltage of photovoltaic module

N_s = no. of PV module connected in series

N_p = no. of PV module connected in parallel

K_i = temp. coefficient of I_{sc}

K_v = temp. coefficient of V_{oc}

G = effective irradiation for PV module

T = temperature of PV module

WPT = wavelet packet transform

STD = standard deviation

References

1. J. F. Mercure and P. Salas, “An assessement of global energy resource economic potentials,” *Energy*, vol. 46, no. 1, pp. 322–336, 2012, doi: 10.1016/j.energy.2012.08.018.
2. Y. Zhao, J. -F. de Palma, J. Mosesian, R. Lyons and B. Lehman, "Line–Line Fault Analysis and Protection Challenges in Solar Photovoltaic Arrays," *IEEE Transactions on Industrial Electronics*, vol. 60, no. 9, pp. 3784-3795, Sept. 2013, doi: 10.1109/TIE.2012.2205355.
3. M. K. Alam, F. H. Khan, J. Johnson, and J. Flicker, “PV faults: Overview, modeling, prevention and detection techniques,” *2013 IEEE 14th Workshop on Control and Modeling for Power Electronics (COMPEL)*, 2013, doi: 10.1109/COMPEL.2013.6626400.
4. M. C. Falvo and S. Capparella, “Safety issues in PV systems: Design choices for a secure fault detection and for preventing fire risk,” *Case Stud. Fire Safety*, vol. 3, pp. 1–16, 2015, doi: 10.1016/j.csfs.2014.11.002.
5. U.S. National Electrical Code, “Article 690—Solar Photovoltaic Systems,” pp. 623–638, 2014, [Online]. Available: https://enkonn-solar.com/wp-content/uploads/2023/08/Article-690-Photovoltaic-PV-System.pdf
6. J. C. Wiles and D. L. King, “Blocking diodes and fuses in low-voltage PV systems,” *Conf. Rec. IEEE Photovolt. Spec. Conf.*, pp. 1105–1108, 1997, doi: 10.1109/pvsc.1997.654281.
7. W. Bower and J. Wiles, “Investigation of ground-fault protection devices for photovoltaic power systems applications,” *Conf. Rec. IEEE Photovolt. Spec. Conf.*, vol. 2000-Janua, no. d, pp. 1378–1383, 2000, doi: 10.1109/PVSC.2000.916149.
8. S. E. Forman, “Performance of Experimental Terrestrial Photovoltaic Modules,” *IEEE Trans. Reliab.*, vol. R-31, no. 3, pp. 235–245, 1982, doi: 10.1109/TR.1982.5221326.
9. D. Stellbogen, "Use of PV circuit simulation for fault detection in PV array fields," Conference Record of the Twenty Third IEEE Photovoltaic Specialists Conference - 1993 (Cat. No.93CH3283-9), Louisville, KY, USA, 1993, pp. 1302-1307, doi: 10.1109/PVSC.1993.346931.
10. S. Fadhel *et al.*, “PV shading fault detection and classification based on I-V curve using principal component analysis: Application to isolated PV system,” *Sol. Energy*, vol. 179, pp. 1–10, 2019, doi: 10.1016/j.solener.2018.12.048.
11. O. W. Yin and B. C. Babu, “Optik Simple and easy approach for mathematical analysis of photovoltaic (PV) module under normal and partial shading conditions,” *Opt. - Int. J. Light Electron Opt.*, vol. 169, no. May, pp. 48–61, 2018, doi: 10.1016/j.ijleo.2018.05.037.
12. M. Gokdag, M. Akbaba, and O. Gulbudak, “Switched-capacitor converter for PV modules under partial shading and mismatch conditions,” *Sol. Energy*, vol. 170, no. June, pp. 723–731, 2018, doi: 10.1016/j.solener.2018.06.010.
13. R. Hariharan, M. Chakkarapani, G. Saravana Ilango and C. Nagamani, "A Method to Detect Photovoltaic Array Faults and Partial Shading in PV Systems," in IEEE Journal of Photovoltaics, vol. 6, no. 5, pp. 1278-1285, Sept. 2016, doi: 10.1109/JPHOTOV.2016.2581478.
14. Z. Mao, Z. Sunan, M. Peng, S. Yanlong, and Z. Weiping, “Macro-model of PV module and its application for partial shading analysis,” *IET Renewable Power Generation*, vol. 12, no. 15, pp. 1748-1754, 2018, doi: 10.1049/iet-rpg.2018.5012.

15. F. Spertino and J. S. Akilimali, “Are manufacturing I-V mismatch and reverse currents key factors in large photovoltaic arrays?,” *IEEE Trans. Ind. Electron.*, vol. 56, no. 11, pp. 4520–4531, 2009, doi: 10.1109/TIE.2009.2025712.

16. H. Patel and V. Agarwal, "Maximum Power Point Tracking Scheme for PV Systems Operating Under Partially Shaded Conditions," *IEEE Transactions on Industrial Electronics*, vol. 55, no. 4, pp. 1689-1698, April 2008, doi: 10.1109/TIE.2008.917118.

17. D. S. Pillai, N. Rajasekar, J. P. Ram, and V. Kumar, “Design and testing of two phase array recon fi guration procedure for maximizing power in solar PV systems under partial shade conditions (PSC),” *Energy Convers. Manag.*, vol. 178, no. June, pp. 92–110, 2018, doi: 10.1016/j.enconman.2018.10.020.

18. H. S. Sahu, S. K. Nayak and S. Mishra, "Maximizing the Power Generation of a Partially Shaded PV Array," *IEEE Journal of Emerging and Selected Topics in Power Electronics*, vol. 4, no. 2, pp. 626-637, June 2016, doi: 10.1109/JESTPE.2015.2498282.

19. M. Dhimish, V. Holmes, B. Mehrdadi, and M. Dales, “Diagnostic method for photovoltaic systems based on six layer detection algorithm,” *Electr. Power Syst. Res.*, vol. 151, pp. 26–39, 2017, doi: 10.1016/j.epsr.2017.05.024.

20. S. Spataru, D. Sera, T. Kerekes, and R. Teodorescu, “Diagnostic method for photovoltaic systems based on light I-V measurements,” *Sol. Energy*, vol. 119, pp. 29–44, 2015, doi: 10.1016/j.solener.2015.06.020.

21. C. Kapucu and M. Cubukcu, “A supervised ensemble learning method for fault diagnosis in photovoltaic strings,” *Energy*, vol. 227, 2021, doi: 10.1016/j.energy.2021.120463.

22. L. Wu *et al.*, “Parameter extraction of photovoltaic models from measured I-V characteristics curves using a hybrid trust-region re fl ective algorithm,” *Appl. Energy*, vol. 232, no. September, pp. 36–53, 2018, doi: 10.1016/j.apenergy.2018.09.161.

23. B. P. Kumar, G. S. Ilango, M. J. B. Reddy and N. Chilakapati, "Online Fault Detection and Diagnosis in Photovoltaic Systems Using Wavelet Packets," *IEEE Journal of Photovoltaics*, vol. 8, no. 1, pp. 257-265, Jan. 2018, doi: 10.1109/JPHOTOV.2017.2770159.

24. S. Silvestre, M. A. Da Silva, A. Chouder, D. Guasch, and E. Karatepe, “New procedure for fault detection in grid connected PV systems based on the evaluation of current and voltage indicators,” *Energy Convers. Manag.*, vol. 86, pp. 241–249, 2014, doi: 10.1016/j.enconman.2014.05.008.

25. A. K. Gupta, M. Gupta, and R. Saxena, “Modeling and Comparative Analysis of PV Module with Improved Perturbation & Observation Based MPPT Technique for PV Applications,” *Arch. Curr. Res. Int.*, vol. 15, no. 1, pp. 1–12, 2018, doi: 10.9734/acri/2018/43457.

26. D. S. Pillai and N. Rajasekar, “An MPPT-based sensorless line-line and line-ground fault detection technique for pv systems,” *IEEE Trans. Power Electron.*, vol. 34, no. 9, pp. 8646–8659, 2019, doi: 10.1109/TPEL.2018.2884292.

27. C. G. Lee *et al.*, “Analysis of electrical and thermal characteristics of PV array under mismatching conditions caused by partial shading and short circuit failure of bypass diodes,” *Energy*, vol. 218, p. 119480, 2021, doi: 10.1016/j.energy.2020.119480.

28. K. Brecl, M. Bokalič, and M. Topič, “Annual energy losses due to partial shading in PV modules with cut wafer-based Si solar cells,” *Renew. Energy*, vol. 168, pp. 195–203, 2021, doi: 10.1016/j.renene.2020.12.059.

29. L. Tang, X. Wang, W. Xu, C. Mu, and B. Zhao, “Maximum power point tracking strategy for photovoltaic system based on fuzzy information diffusion under partial shading conditions,” *Sol. Energy*, vol. 220, no. April, pp. 523–534, 2021, doi: 10.1016/j.solener.2021.03.047.

30. R. Hariharan, M. Chakkarapani, G. Saravana Ilango, and C. Nagamani, “A Method to Detect Photovoltaic Array Faults and Partial Shading in PV Systems,” *IEEE J. Photovoltaics*, vol. 6, no. 5, pp. 1278–1285, 2016, doi: 10.1109/JPHOTOV.2016.2581478.

31. M. Dhimish, V. Holmes, B. Mehrdadi, and M. Dales, “Simultaneous fault detection algorithm for grid-connected photovoltaic plants,” *IET-Renewable Power Generation*, vol. 11, no. 12, pp. 1565–1575, 2017, doi: 10.1049/iet-rpg.2017.0129.

32. Z. Chen, L. Wu, S. Cheng, P. Lin, Y. Wu, and W. Lin, “Intelligent fault diagnosis of photovoltaic arrays based on optimized kernel extreme learning machine and I-V characteristics,” *Appl. Energy*, vol. 204, pp. 912–931, 2017, doi: 10.1016/j.apenergy.2017.05.034.

33. B. P. Kumar, G. S. Ilango, M. J. B. Reddy, and N. Chilakapati, “Online fault detection and diagnosis in photovoltaic systems using wavelet packets,” *IEEE J. Photovoltaics*, vol. 8, no. 1, pp. 257–265, 2018, doi: 10.1109/JPHOTOV.2017.2770159.

34. J. M. Huang, R. J. Wai, and W. Gao, “Newly-designed fault diagnostic method for solar photovoltaic generation system based on IV-Curve measurement,” *IEEE Access*, vol. 7, pp. 70919–70932, 2019, doi: 10.1109/ACCESS.2019.2919337.

35. Y. Liu *et al.*, “Fault diagnosis approach for photovoltaic array based on the stacked auto-encoder and clustering with I-V curves,” *Energy Convers. Manag.*, vol. 245, 2021, doi: 10.1016/j.enconman.2021.114603.

.

□❍□